International Journal of Physical Sciences Vol. 4 (12), pp. 743-751, December, 2009
Available online at http://www.academicjournals.org/ijps
ISSN 1992 - 1950 © 2009 Academic Journals

Full Length Research Paper

The application of artificial neural networks technique to estimate mass attenuation coefficient of shielding barrier

Osman Gencel

Department of Civil Engineering, Faculty of Engineering, Bartin University, 74100 Bartin, Turkey. E-mail: osmangencel@gmail.com.

Accepted 20 November, 2009

This study aims to investigate comparison of radiation attenuation property of harzburgite mineral calculated by Monte Carlo (MCNP) and Artificial Neural Network (ANN). Slab sample modeled in MCNP with 1, 2 and 4 cm thickness was irradiated with parallel beam of monoenergetic particles. Incoming and outgoing particle fluxes were computed with F1 tally. Beer-Lambert equation was used to obtain mass attenuation coefficients for photon energies between 40 keV and 20 MeV. Optimum ANN model was obtained after trying different structures in terms of iterations and hidden layer numbers. For ANN calculation, parameters considered in the study are dose, thickness and mass attenuation coefficient. Dose and thickness are used as inputs to ANN for the estimation of mass attenuation coefficient. Model results are evaluated using root mean square errors (RMSE) and determination coefficient (R^2) statistics. The estimates of selected ANN model were compared with MCNP results. Based on the comparison results, ANN was found good in prediction of mass attenuation coefficient for shielding material. Relationship between observed MCNP values and ANN estimates is noticeable with a high determination coefficient (R^2) of 1 and has a root mean square error (RMSE) of 0.0033.

Key words: Monte Carlo, artificial neural network, mass attenuation coefficient, radiation shielding.

INTRODUCTION

Many types of radiation, such as neutron and x-ray or photon, cause ionization of the media with which they interact, through a complicated mechanism involving the emission of energetic secondary charged particles. The ionizing ability of these types of radiation is the reason for the importance of studying shields. A shield is physical entity interposed between a source of ionizing radiation and an object to be protected, such that the radiation level at the position of the object will be reduced. The object to be protected is most often a human being, but it can be anything that is sensitive to ionizing radiation (Abdel-Aziz et al., 1995).

There are many types of radiation and different ways and methods and materials to be protected from them have been used. For instant, to be protected from cosmic radiation containing many types of radiation with widely varying energies or radiation like ultraviolet A, B and C from the sun, lotion and sun glasses is used. But they can't be used for walls of the nuclear power plant and radiotherapy rooms to stop radiation.

Many materials have been used for this purpose. One of these materials has been concrete. Concrete is considered to be an excellent and versatile shielding material; it is widely used for shielding nuclear power plants, particle accelerators, research reactors, laboratory hot cells and medical facilities. Concrete is a relatively inexpensive material, it can be easily handled and cast into complex shapes. It contains a mixture of various light and heavy elements and a capability for attenuation of photon and neutrons. By varying its composition and density and thickness the shielding characteristics of concrete may be adapted to a wide range of uses (Kaplan, 1989).

As well radiation shielding, to measure or test linear attenuation coefficient (μ) and then total mass attenuation coefficients (μ/ρ) of material has importance. The linear attenuation coefficient is the probability of a photon interacting a particular way with a given material, per unit path length this coefficient is of great importance in matters concerning radiation shielding and its dimension. The mass attenuation coefficient (μ/ρ) is a measure of the average number of interactions between incident photons and matter that occur in a given mass-per unit area

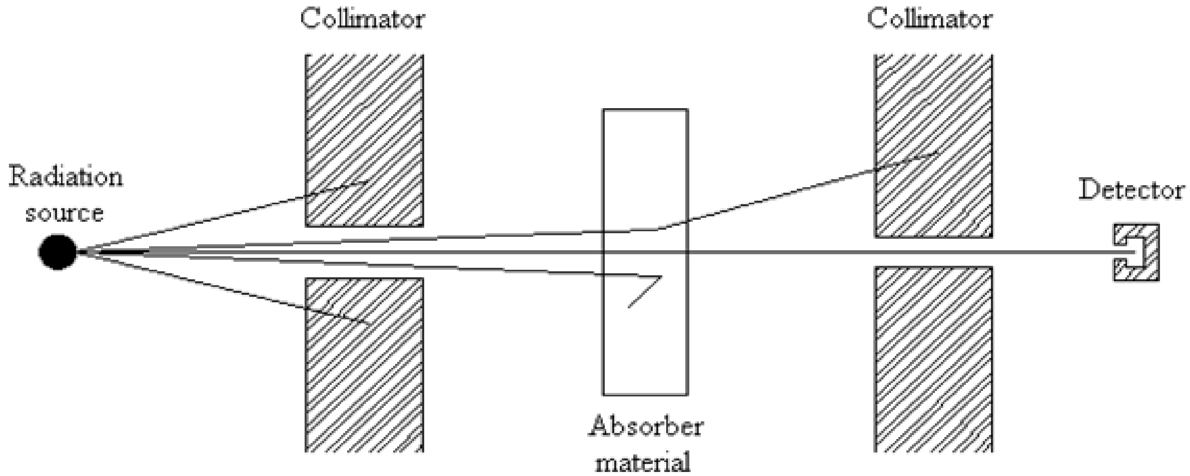

Figure 1. Schematic view of setup and collimations first method.

thickness of the substance under investigation and direct measure the effectiveness of a shielding (Wood, 1982).

Accepted three methods have been used for it. First one is physical test method. In this method, as shown in Figure. 1 the radioactive sources are shielded by the pin hole lead collimators to obtain a narrow beam. This form of narrow-beam experimental arrangement is called as good geometry. Also the detector is shielded by a lead collimator. The source-sample and sample-detector distance is set. Besides, the test room must be well-shielded.

In this method, there are some noted difficulties follows; 1) Sources and detector is collimated to obtain a narrow beam. 2) If monoenergetic photons are considered for application, monoenergetic photons can't always be produced. 3) The facilities to fulfill this test cannot be common. 4) For this method, we must have a sample produced, in case of getting insufficient result from test, go back and produce material again. It seems as waste of time, energy and materials. 5) And importantly, the measurement can be repeated a few times, this seems problem in point of improving the statistical error.

Second one is biological method. In this method, biological objects (rat, blood, tissue etc.) are used. In the study of Gencel (Gencel et al., in press), rats were housed in concrete-protected cages and then irradiated (Figure 2). Thus, protective effect of shielding material is determined by dependent on effect of radiation on rat tissue. This method also seems hard since it needs interdisciplinary cooperation.

The third one is simulation. The simulation has advantage on first and second methods in point of difficulties mentioned above. Monte Carlo, XCOM, MERCSF-N and some other simulation programs have been used. But, Monte Carlo and XCOM are very famous of them and used and accepted all around the world.

The calculation of the mass attenuation coefficients for different building materials have been performed with a computer program developed by Berger and Hubbel called XCOM (Berger and Hubbel, 1987).

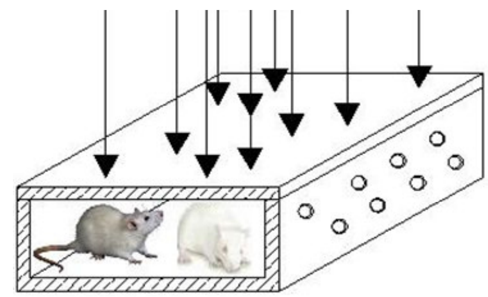

Figure 2. Experimental setup of concrete-protected cage for second method.

Artificial Neural Networks (ANN) can supply meaningful answers even when the data to be processed include errors or are incomplete and can process information extremely rapidly when applied to solve engineering problems (Topcu and Saridemir, 2007; Lippman, 1987). Therefore, ANN have been used for many applications in various areas like environmental, biological, social, computer, earth, energy, civil and material sciences engineering. However, very little study has been conducted about ANN for radiation shielding of materials. In this study, we aimed to investigate usage of ANN for this purpose by comparison with Monte Carlo.

MATERIALS AND SIMULATION

Monte Carlo method

The Monte Carlo method is a numerical solution to a problem that models objects interacting with other objects or their environment based upon simple object-object or object environment relation-

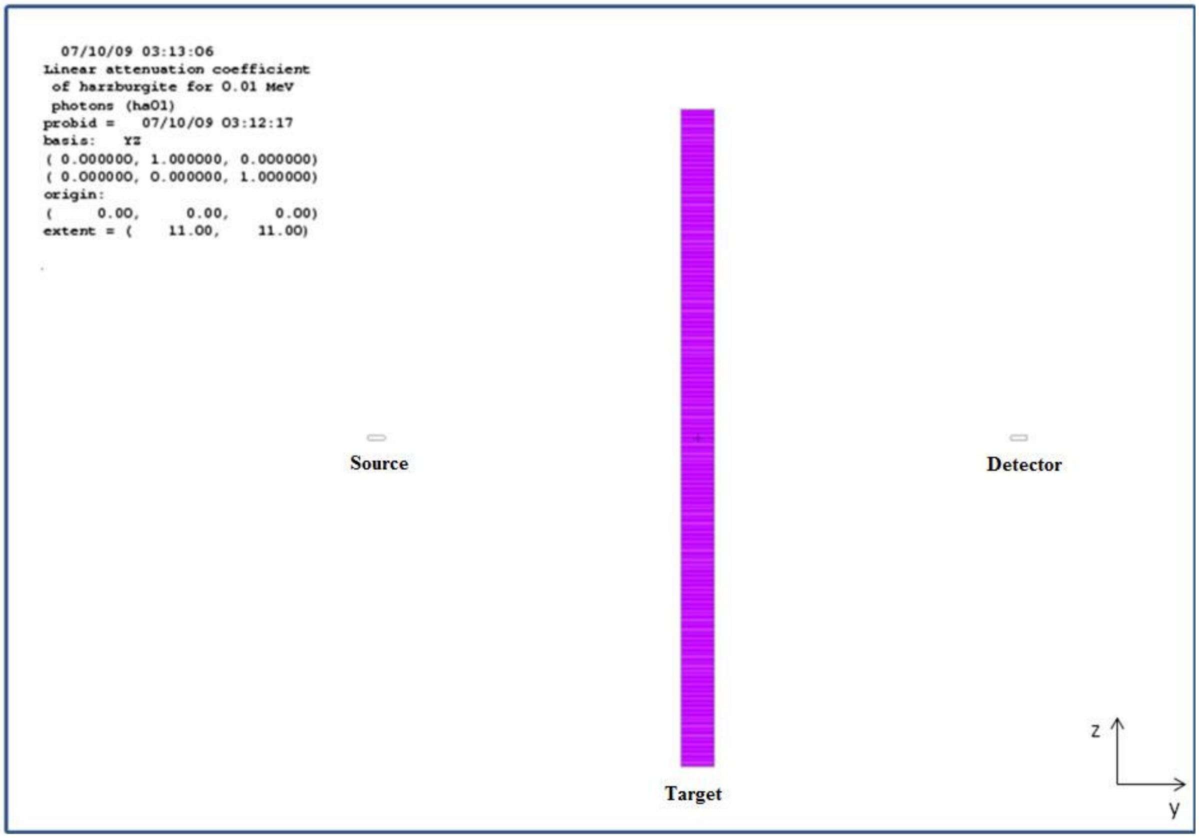

Figure 3. Experimental geometry modeled with Monte Carlo.

ships. There are many examples of the use of the Monte Carlo method that can be drawn from social science, traffic flow, population growth, finance, genetics, quantum chemistry, radiation sciences, radiotherapy, and radiation dosimetry. But, these works will concentrate on the simulation of photons being transported in condensed materials (Bielajew, 2001).

In order to decide whether a Monte Carlo method should be applied to a given problem, it is reasonable to see how it compares with other available methods. In the case of integration, alternative numerical techniques have been the subject of extensive studies for centuries, and the widespread use of computers has led to considerable practical experience in this field (James, 1980).

There is no need to argue about MCNP for this application. The literature is very rich in works dealing mass attenuation coefficients of materials. This method modeling interaction radiation with matter calculates particle energy, position, direction, travel and appropriate probability distributions and thus tries to estimate energy loss in each interaction and at the end it calculate absorbed radiation doses in the matter described in volume.

With Monte Carlo code (Briesmeister, 2000), a point source in an empty space was modeled and the photons were transported from the source to a detector. Between detector and source the material shielding was put. Source-sample and sample-detector distance was 20 cm as seen in Figure 3.

The density (ρ) and photon energy are the main parameters that affect the mass attenuation calculations.

A shield material (rho, ρ, = 4 g/cm^3) with slab geometry modeled in MCNP was irradiated with monoenergetic parallel beam coming the source. Particle fluxes were calculated with F1 tally of MCNP for energies between 40 keV and 20 MeV for harzburgite mineral. And then the attenuation coefficients were measured by using Beer-Lambert's law:

$$I = I_0 e^{-\mu\chi} \tag{1}$$

Where x is the thickness of the sample under study, I_0 is the number of counts representing the intensity of incident gamma-ray photons, at a specific energy, without attenuation and I is the gamma-ray counts that penetrated the absorber with attenuation in the sample. More conveniently, a coefficient that is density independent is the mass attenuation coefficient, defined as μ/ρ (cm^2/g).

$$\mu / \rho = -\frac{1}{\rho\chi} \ln\left(\frac{I}{I_0}\right) \tag{2}$$

In this study, harzburgite as absorber material was used. Harzburgite is a green colored and fine-grained igneous rock consisting of olivine (mostly 70 - 90%), pyroxene with low-calcium (little10 - 30%) and chromite (minor 1 - 2%) minerals. Harzburgite is the dominant rock of the upper part (30-200 km) of the Earth's mantle. Harzburgites are commonly derived from the upper mantle by partial melting of mantle peridotites (Blatt et al., 1996). Polarize microscope view is presented in Figure 4. Elemental composition of harzburgite mineral used is given in Table 1.

Artificial Neural Networks (ANN)

Artificial neural networks (ANN) are a functional abstraction of the

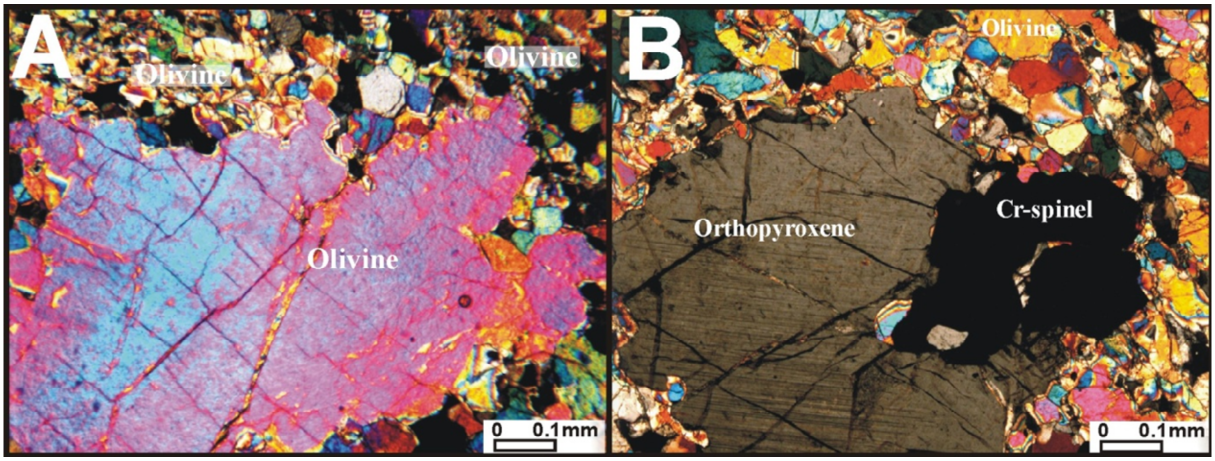

Figure 4. The microscopical views from the harzburgite showing porphyroclastic texture. Olivine (A) and orthopyroxene (B) porphyroclasts are observed as corroded along their boundaries within anhedral olivine. Olivines included by chrome spinel and orthopyroxene.

Table 1. Elemental composition of harzburgite.

Element	O	Mg	Al	Si	P	Ca	Cr	Mn	Fe	Ni
Weight (%)	44.4	26.4	0.418	20.8	0.013	0.529	0.288	0.093	6.0	0.223

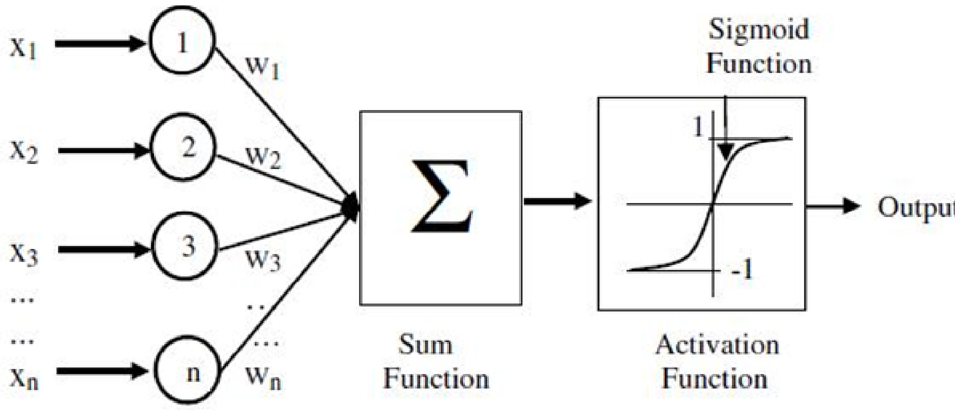

Figure 5. A simple neuron model.

biological neutral structures of the central nervous system (Anderson, 1983; Gunaydın and Dogan, 2004; Arbib, 1995; Anderson, 1995), though much of the biological detail is neglected (Lippman, 1987). The first studies on ANN are supposed to have started in 1943. McCulloch and Pitts defined artificial neurons for the first time and developed a cell model as in Figure 5 (Topcu and Saridemir, 2007). After this earliest and most basic model, many complex neural net applications and mechanisms have been shown up. As a result of these studies and developments in computer technology, use of ANN has become more efficient in 1980s (Topcu and Saridemir, 2007; Anderson, 1995).

ANN is massively parallel systems composed of many processing elements connected by links of variable weights (Lippman, 1987). A weight is assigned to each connection which can be adjusted in such a manner when a set of inputs is given to the network, the associated connections will produce a desired output (Topcu and Saridemir, 2007). Of the many ANN paradigms, the multi-layer back propagation network (MLP) has been by far the most popular learning algorithms (Lippman, 1987). Among various architectures and paradigms, the back propagation networks being used in performing higher level of human task such as diagnosis, classification, decision-making, planning and scheduling (Sohabhon and Spethen, 1999). The network consists of layers of parallel processing elements, called neurons, with each layer being fully connected to the proceeding by interconnection strengths, or weights (W). Figure 6 illustrates a three-layer neural network consisting of layers i, j, and k, with the interconnection weights W_{ij} and W_{jk} between layers of neurons. The process of determining ANN weights is called learning or training and is similar to the calibration of a mathematical model. The ANN are trained with a training set of input and known output data. At the beginning of training, the weights are initialized, either with a set of random values or based on some previous experience. Initial estimated

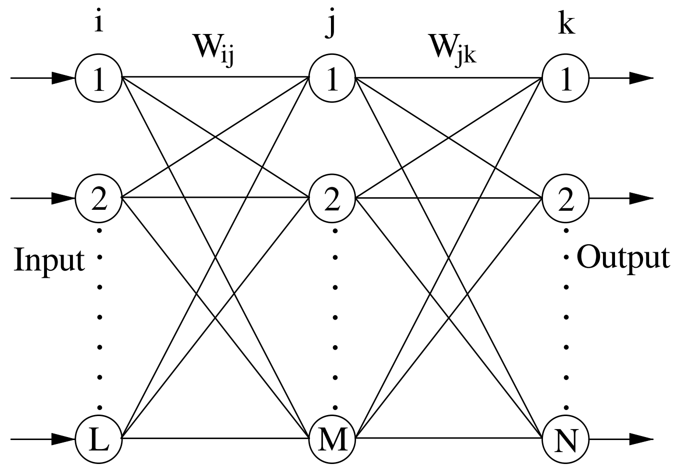

Figure 6. Plot of observed MCNP and predicted μ/ρ by ANN.

weight values are progressively corrected during a training process that compares predicted outputs to known outputs, and back propagates any errors (from right to left in Figure 6) to determine the appropriate weight adjustments necessary to minimize the errors. At this stage, the ANN is considered trained.

The Levenberg-Marquardt training algorithm (Marquardt, 1963; Hagan and Menhaj, 1994) was used here for adjusting the weights. The adaptive learning rates were used for the purpose of faster training speed and solving local minima problem. For each epoch, if performance decreases toward the goal, then the learning rate is increased by the factor learning increment. If performance increases, the learning rate is adjusted by the factor learning decrement. The numbers of hidden layer neurons were found using simple trial-error method.

Application of ANN and results

A program code including neural networks toolbox, were written in MATLAB language for the ANN simulation. Different ANN architectures were tried using this code and the appropriate model structure was determined.

A difficult task with ANN involves choosing parameters such as the number of hidden nodes, the learning rate, and the initial weights. Determining an appropriate architecture of a neural network for a particular problem is an important issue, since the network topology directly affects its computational complexity and its generalization capability. The optimum network geometry is obtained utilizing a trial-and-error approach in which ANN are trained with one hidden layer. It should be noted that one hidden layer could approximate any continuous function, provided that sufficient connection weights are used (Hornik et al., 1989). Here, the hidden layer node number of ANN model was determined after trying various network structures since there is no theory yet to tell how many hidden units are needed to approximate any given function. In the training stage, the same initial weights were used for each ANN networks. The sigmoid activation function was used for the hidden and output nodes (Kocabas et al., 2008, 2009).

The parameters considered in the study are the dose, thickness and mass attenuation coefficient (μ/ρ). The parameters the dose and thickness are used as inputs to the ANN for the estimation of mass attenuation coefficient. Of the 99 experimental data sets, the 60 data are used to train the ANN and the remaining data are used for validation. The remaining 39 data sets are randomly selected among the whole data. The model results are evaluated using root mean square errors (RMSE) and determination coefficient (R^2) statistics. These are defined as,

$$RMSE = \sqrt{\frac{1}{n}\sum_{i=1}^{n}\left\{(\mu/\rho)_{MCNP,i} - (\mu/\rho)_{ANN,i}\right\}^2} \tag{3}$$

$$R^2 = \frac{\sum_{i=1}^{n}\left\{(\mu/\rho)_{MCNP,i} - \overline{(\mu/\rho)}_{MCNP}\right\}^2 - \sum_{i=1}^{n}\left\{(\mu/\rho)_{MCNP,i} - (\mu/\rho)_{ANN,i}\right\}^2}{\sum_{i=1}^{n}\left\{(\mu/\rho)_{MCNP,i} - \overline{(\mu/\rho)}_{MCNP}\right\}^2} \tag{4}$$

RMSE measure residual errors give a global idea of the difference between the observed and modeled values. And R^2 provides the variability measure of the data reproduced in the model. $\overline{(\mu/\rho)}_{MCNP}$ is the average of $(\mu/\rho)_{MCNP,i}$.

Before applying the ANN to the data, the training input and output values were normalized using the equation:

$$a\frac{x_i - x_{\min}}{x_{\max} - x_{\min}} + b \tag{5}$$

Where $x_{\min}$ and $x_{\max}$ denote the minimum and maxi-

Table 2. The RMSE statistics obtained after different trials.

RMSE		Iteration Number					
		50	100	150	200	250	300
Number of hidden layer nodes	1	0.0438	0.0437	0.0437	0.0436	0.0436	0.0436
	2	0.0437	0.0437	0.0437	0.0436	0.0436	0.0436
	3	0.0041	0.0034	0.0033	0.0033	0.0034	0.0034
	4	0.0419	0.0074	0.0055	0.0049	0.0046	0.0045
	5	0.0050	0.0048	0.0048	0.0048	0.0048	0.0048
	6	0.0049	0.0048	0.0047	0.0047	0.0047	0.0047
	7	0.0057	0.0058	0.0068	0.0069	0.0069	0.0068
	8	0.0064	0.009	0.0083	0.0086	0.0087	0.0090
	9	0.0044	0.0045	0.0047	0.0048	0.0048	0.0049
	10	0.0077	0.0079	0.0083	0.0111	0.0121	0.0160

Table 3. Comparison of μ/ρ obtained by MCNP and ANN for different energies.

Energy (MeV)	t = 1 cm		t = 2 cm		t = 4 cm	
	ANN	MCNP	ANN	MCNP	ANN	MCNP
0.05	0.400440	0.400642	0.400729	0.400834	0.401316	0.401275
0.07	0.245682	0.244555	0.245407	0.245255	0.244861	0.245389
0.1	0.179499	0.178389	0.179053	0.178395	0.178164	0.178652
0.3	0.107823	0.107404	0.107326	0.107094	0.106346	0.107206
0.6	0.080303	0.080307	0.079890	0.080193	0.079085	0.080017
0.8	0.070204	0.070409	0.069844	0.070367	0.069149	0.070141
1.25	0.056324	0.056327	0.056061	0.056408	0.055559	0.056245
1.75	0.047479	0.047520	0.047291	0.047508	0.046939	0.047361
4	0.031809	0.031683	0.031785	0.031617	0.031760	0.031633
6	0.026917	0.026643	0.026955	0.026571	0.027053	0.026597
9	0.023469	0.023382	0.023557	0.023358	0.023754	0.023354
12	0.021733	0.021796	0.021852	0.021806	0.022108	0.021826
18	0.020091	0.020264	0.020246	0.020362	0.020576	0.020463

mum of the data. Different values can be assigned for the scaling factors a and b. There are no fixed rules as to which standardization approach should be used in particular circumstances (Dawson and Wilby, 1998). Range of 0.2 - 0.8 increases the extrapolation ability of the ANN models (Cigizoglu, 2003; Kisi, 2008; Kisi and Cobaner, 2009). Therefore, in this study the a and b were taken as 0.6 and 0.2, respectively.

Different ANN structures are tried in terms of iterations and hidden layer numbers. The test RMSE statistics of the ANN models are given in Table 2. The best one that gave the minimum root mean square errors (RMSE) was selected. As can be seen from this table, the ANN (2, 3 and 1) model comprising 2 input, 3 hidden and 1 output layer neurons has the lowest RMSE (0.0033). Mass attenuation coefficient obtained by both MCNP and ANN for different energies is presented in Table 3.

The relationship between MCNP observation of μ/ρ and predicted μ/ρ by ANN is linear as shown in Figures 7, 8 and 9 for 1, 2 and 4 cm thickness, respectively.

The relationship between observed μ/ρ and predicted μ/ρ by ANN for t = 1, 2 and 4 cm is also linear as shown in Figure 10. The fit line equation coefficients of the ANN model, 0.9997 and 5E-5, are closer to the 1 and 0, respectively. The relationship between the observed values and the ANN model predictions is noticeable with correlation of $R^2 = 1$.

Observed μ/ρ values and predictions by ANN are shown in Figure 11. As can be seen from Figure 11, the ANN estimates catch the MCNP values with a high accuracy.

Conclusion

Artificial Neural Network (ANN) model was used for analysis of MCNP results in the present study. The optimum ANN model was obtained after trying different structures in terms of iterations and hidden layer numbers. The estimates of the selected ANN model were

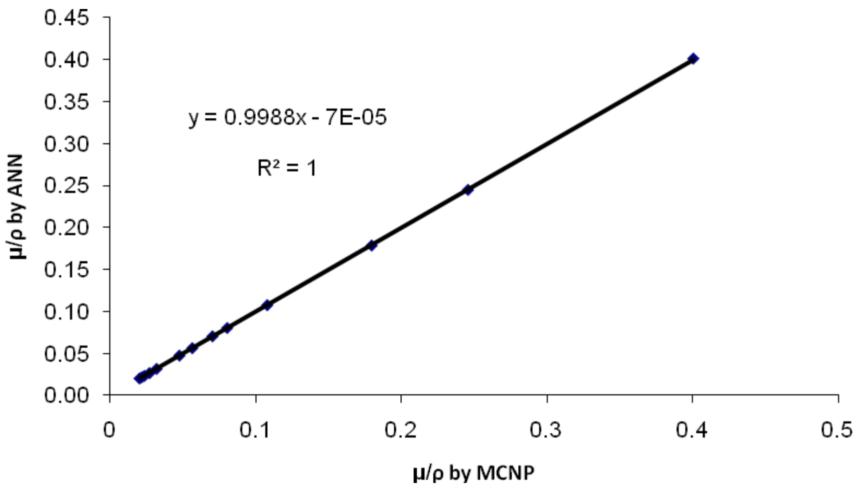

Figure 7. Comparison of μ/ρ calculated by MCNP and ANN for 1 cm material thickness.

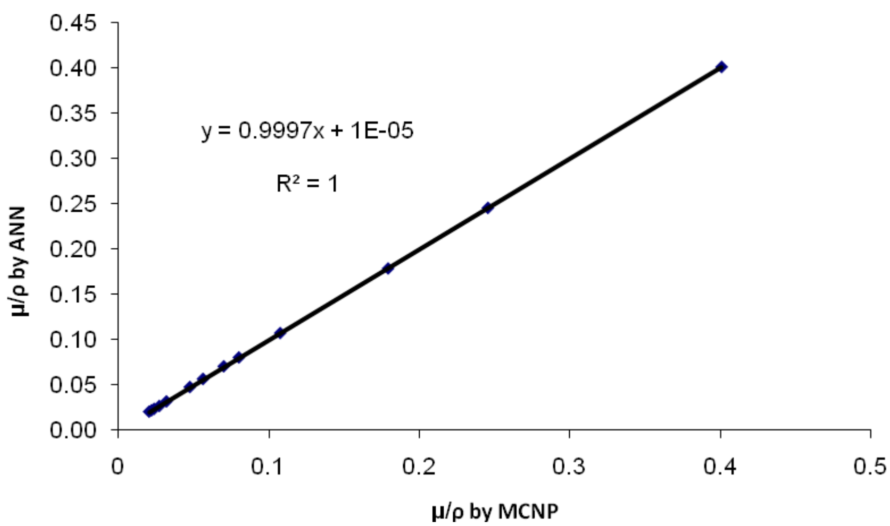

Figure 8. Comparison of μ/ρ calculated by MCNP and ANN for 2 cm material thickness.

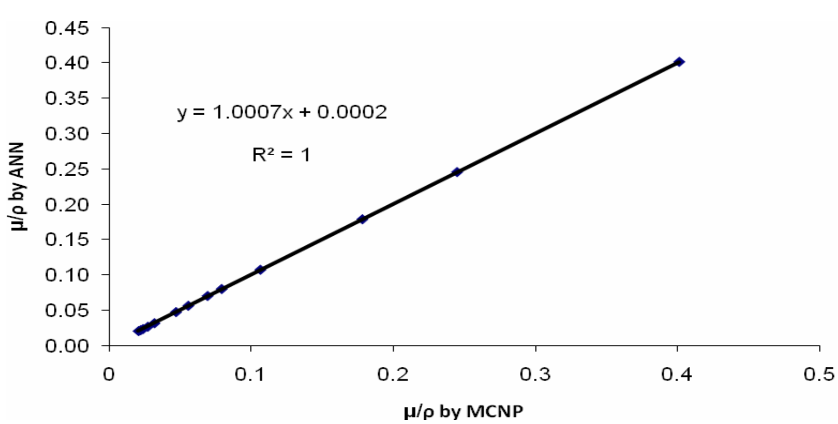

Figure 9. Comparison of μ/ρ calculated by MCNP and ANN for 4 cm material thickness.

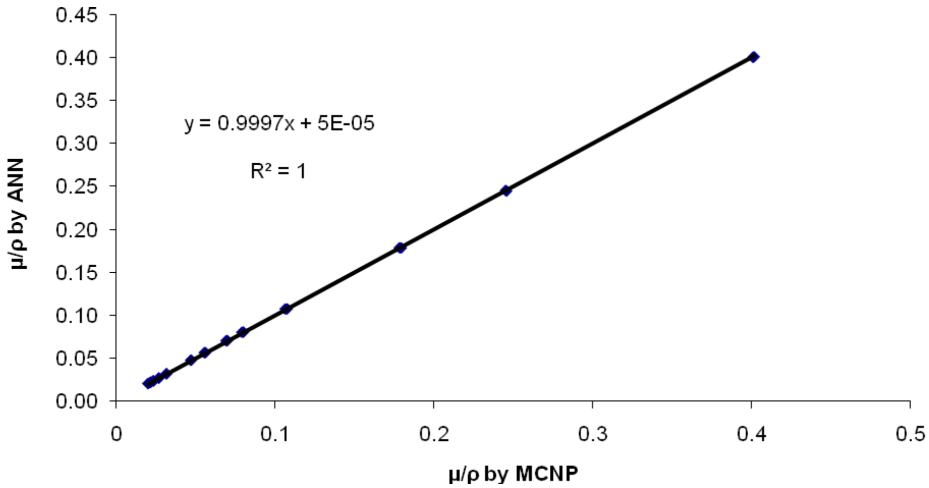

Figure 10. General comparison between MCNP and ANN for μ/ρ.

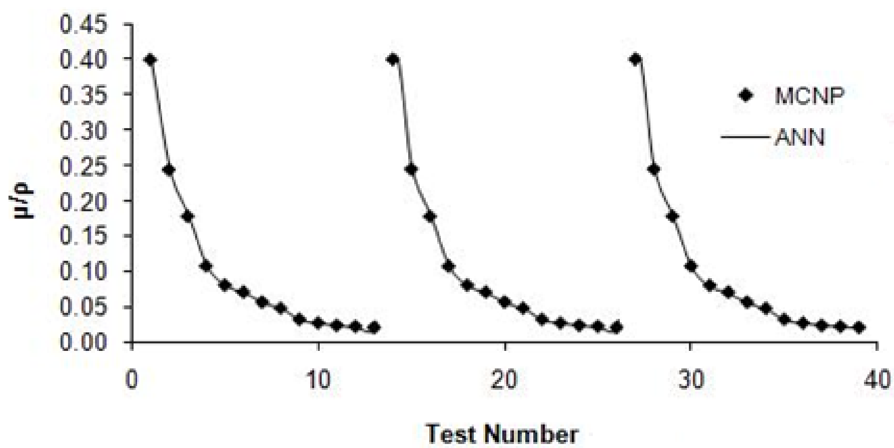

Figure 11. MCNP Observations and predicted μ/ρ by ANN.

compared with the MCNP results. Based on the comparison results, the ANN was found good in prediction of mass attenuation coefficient for a shielding material. The relationship between the MCNP values and the ANN estimates is noticeable with a high determination coefficient (R^2) of 1 and has a root mean square error (RMSE) of 0.0033.

REFERENCES

Abdel-Aziz MM, Gwaily SE, Makarious AS, El-Sayed Abdo A (1995). Ethylene-proplene diene rubber/low density polyethylene/boron carbide composites as neutron shields. Polym. Degrad. Stability 50: 235-240.

Anderson JA (1983). Cognitive and psychological computation with neural models, IEEE Transactions on Systems, Man Cybernetics 5: 799–814, V.SMC-13.

Anderson JA (1995). An introduction to computing with neural nets, A Bradford book, MIT Press, Cambridge (MA).

Arbib MA (1995). The Handbook of Brain Theory and Neural Networks, MIT Press, Cambridge (MA).

Berger MJ, Hubbel JH (1987). XCOM: photon cross sections on a personal computer. NBSIR 87: 3597-3598.

Bielajew AF (2001). Fundamentals of the Monte Carlo method for neutral and charged particle transport, The university of Michigan, September 17.

Blatt H, Robert JT (1996). Petrology: Igneous, Sedimentary and Metamorphic, 2nd ed., Freeman.

Briesmeister JF (2000). MCNP-A general Monte Carlo N-particle transport code, Version 4C. Technical Report No. LA-13709-M, Los Alamos National Laboratory, New Mexico.

Cigizoglu HK (2003). Estimation, forecasting and extrapolation of river flows by artificial neural networks. Hydrol. Sci. J., 48(3): 349-361.

Dawson WC, Wilby R (1998). An artificial neural network approach to rainfall-runoff modeling. Hydrol. Sci. J. 43(1): 47-66.

Gencel O, Naziroglu M, Celik O, Yalman K, Bayram D, Selenium and vitamin E Modulates Radiation-Induced Liver Toxicity in Pregnant and Nonpregnant Rat: Effects of Colemanite and Hematite Shielding. Biol. Trace Elem. Res. (In press).

Gunaydın HM, Dogan SZ (2004). Int. J. Proj. Manage. 22(7): 595–602.

Hagan MT, Menhaj M (1994). Training feed forward networks with the

Marquardt algorithm. IEEE Transactions on Neural Networks, 5(6): 989-993.
Hornik K, Stinchcombe M, White H (1989). Multilayer feedforward networks are universal approximators. Neural Networks, 2: 359-366.
James J (1980). Monte Carlo theory and practice. Rep. Prog. Phys. 43.
Kaplan MF (1989). Concrete Radiation Shielding, Wiley, New York, USA.
Kişi Ö (2008). Daily pan evaporation modelling using multi-layer perceptrons and radial basis neural Networks. Hydrol. Proces. 23(2): 213-223.
Kişi Ö, Çobaner M (2009). Modeling River Stage-Discharge Relationships Using Different Neural Network Computing Techniques. Clean-Soil-Air-Water 37(2): 160-169.
Kocabaş F, Kişi Ö, Ardıçlıoğlu M (2009). An artificial neural network model for prediction of critical submergence for an intake in a stratified fluid media. Civil Eng. Environ. Syst. 26(4): 367-375.
Kocabaş F, Ünal S, Ünal B (2008). A neural network approach for prediction of critical submergence of an intake in still water and open channel flow for permeable and impermeable bottom. Comput. Fluids 37: 1040-1046.
Lippman RP (1987). An introduction to computing with neural nets. IEEE ASP Mag. 4-22.
Marquardt D (1963). An algorithm for least squares estimation of non-linear parameters. J. Soc. Ind. Appl. Math. pp. 431-441.
Sohabhon B, Spethen OO (1999) Engineering Construct Architect Manage. 6(2): 133–144.
Topcu IB, Sarıdemir M (2007). Prediction of properties of waste AAC aggregate concrete using artificial neural network, Comput. Mater. Sci. 41: 117–125.
Wood J (1982). Computational Methods in Reactor Shielding, Pergamon Press, Inc., New York, USA.